Plant Hormones ARTICLE

Open Access

https://doi.org/10.48130/ph-0026-0018

Plant Hormones **2026**, 2: e021

Salicylic acid-induced phenolic metabolism enhances apple's resistance to postharvest blue mold

Jianyi Zhang[1], Ning Ma[2], Zhiyi Ji[1] and Youming Shen[1*]

[1] *Research Institute of Pomology, Chinese Academy of Agricultural Sciences, Xingcheng, Liaoning 125100, China*

[2] *College of Veterinary Medicine, Veterinary Biological Technology Innovation Center of Hebei Province, Hebei Agricultural University, Baoding, Hebei 071000, China*

* Correspondence: shenyouming@caas.cn (Shen Y)

Abstract

Postharvest blue mold decay of apples (*Malus domestica*) caused by *Penicillium expansum* infection results in substantial fruit and economic damage. Salicylic acid (SA), a common plant-defense priming agent, enhances disease resistance in apples; however, the metabolic reprogramming underlying this SA-induced defense remains poorly characterized. In this study, we used untargeted metabolomics based on ultrahigh-performance liquid chromatography coupled with quadrupole time-of-flight mass spectrometry (UPLC-Q-TOF/MS) to profile metabolic alterations in apple fruits following SA treatment and *P. expansum* infection. In total, 103 secondary metabolites were differentially abundant across five comparison groups. Enrichment analysis revealed pronounced upregulation of biosynthesis pathways, notably those of flavonoids, phenylpropanoids, flavones, and flavonols. Targeted phenolic profiling further demonstrated that several key phenolics, including procyanidins B1/B2 and chlorogenic acid, significantly increased in abundance during infection, suggesting their potential role in inhibiting disease progression. These findings elucidate the metabolic landscape reshaped by SA treatment in response to *P. expansum* infection, providing novel insights into the metabolic basis of disease defense in apple. The study also highlights phenolic compounds as potential metabolic markers, supporting the development of metabolite-guided strategies for postharvest disease management.

Keywords: *Malus domestica*, Salicylic acid, *Penicillium expansum*, Metabolism, Metabolomics

Citation: Zhang J, Ma N, Ji Z, Shen Y. 2026. Salicylic acid-induced phenolic metabolism enhances apple's resistance to postharvest blue mold. *Plant Hormones* 2: e021 https://doi.org/10.48130/ph-0026-0018

Introduction

Apples (*Malus domestica*) are globally valued for their appealing flavor, rich cultural heritage, and health-promoting nutrients such as vitamins, polyphenols, and dietary fiber[1,2]. However, fresh apples are highly susceptible to fungal infection during storage, leading to postharvest decay and estimated losses of 20%–30% of annual production[3,4]. Among these diseases, blue mold caused by *Penicillium expansum* infection is one of the most prevalent postharvest diseases in apples. *P. expansum* also produces the mycotoxin patulin during the disease's progression, posing a significant risk of mycotoxin contamination of fruit-derived products, which further poses a toxicological threat to human health[5]. Current postharvest fruit sanitation measures and fungicide applications have effectively reduced the incidence of blue mold by suppressing fungal infection and growth. Nevertheless, the misuse of fungicides poses significant risks to consumers' health and environmental safety[6]. This underscores the urgent need to develop eco-friendly and sustainable strategies for postharvest disease management in apple.

Salicylic acid (SA), a natural phenolic compound and endogenous phytohormone, serves as an important resistance inducer in plants[7,8]. As a safe and eco-friendly elicitor, exogenous SA application enhances disease resistance in postharvest fruit, offering a sustainable solution for postharvest preservation, for example, in controlling blue mold in apple[8]. The regulatory mechanisms of SA-induced resistance may operate at multiple levels, involving gene expression, protein function, and metabolic reprogramming[9,10]. As a signalling molecule, SA can bind to functional proteins such as NPR1, subsequently activating downstream signaling cascades that lead to the induction of defense-related genes and the corresponding biochemical responses[11,12]. This regulation promotes critical metabolic shifts that facilitate adaptation to new physiological conditions and that underpin enhanced disease resistance[13,14]. These shifts include the upregulation of pivotal metabolic pathways that are essential for defense, such as the tricarboxylic acid (TCA) cycle, reactive oxygen species metabolism, secondary metabolite biosynthesis, and sphingolipid metabolism[8,14]. However, the systemic metabolic response in apple fruit to SA treatment, particularly the transformation of key functional compounds and the dynamics of their associated pathways, remains inadequately understood.

Our previous studies demonstrated that apple fruit exhibit global metabolic changes in response to SA treatment, indicating that metabolic reprogramming contributes significantly to enhanced disease resistance[15]. Nevertheless, the dynamics of key metabolites involved in SA-enhanced resistance processes are still incompletely understood. Moreover, the fruit's disease resistance is also influenced by intrinsic factors such as the genetic cultivar and physiological maturity, which are frequently overlooked[13,16]. The present study builds upon this foundation by investigating the metabolic mechanisms underlying SA-enhanced blue mold disease resistance in apples. We hypothesize that SA specifically modulates the phenylpropanoid metabolic pathway, leading to the accumulation of disease-resistant phenolic compounds and subsequently reducing disease progression. The specific objectives are (1) to elucidate how SA enhances apple's resistance to blue mold by modulating host's secondary metabolism, (2) to determine temporal changes in the absolute concentrations of representative metabolites, and (3) to characterize metabolic markers associated with induced resistance across a broad spectrum of fruit resources and *P. expansum* strains. These findings are expected to advance our understanding of SA-induced apple disease resistance and provide a theoretical basis for improving postharvest disease-control strategies.

Materials and methods

SA treatment and *P. expansum* inoculation of apples

The *P. expansum* strain was isolated from a typical blue mold lesion on apple and purified on potato dextrose agar (PDA) medium (Aoboxing Biotech Co. Ltd., Beijing, China). For long-term storage, *P. expansum* spores were suspended in 20% glycerol (Coolaber Science and Technology Co., Ltd., Beijing, China) and maintained at −80 °C. For fruit inoculation, *P. expansum* spores were suspended in sterile water to a concentration of 1×10^5 spores/mL.

'Fuji' apples were harvested from the Hot Spring Experimental Base of the Pomology Research Institute, Chinese Academy of Agricultural Sciences, and stored at 0 ± 0.5 °C until use. In total, 72 uniform, healthy fruits were selected and randomly assigned to three groups: SA-treated and infected, the infected (positive) control, and the uninfected (negative) control. Each group comprised eight replicates, with three fruits per replicate. Following the method described previously, fruits in the SA-treated group were immersed in a 5 mM SA solution at 22 °C for 30 min, whereas both control groups were treated with sterile water under identical conditions[15]. After natural drying, two symmetrical wounds were created on opposite sides of each fruit using a sterile lancet to a depth of 3 mm and a width of 2 mm. In the SA-treated and positive control groups, each wound was inoculated with 10 μL of the *P. expansum* spore suspension (1×10^5 spores/mL). Wounds on fruits in the negative control group received 10 μL of sterile water. All inoculated fruits were subsequently incubated at 25 °C and 95% relative humidity. The lesions' diameters were measured daily after inoculation.

Sample collection and untargeted metabolomic analysis

For metabolomic analysis, each treatment group comprised eight biological replicates, each consisting of six tissue samples (two per fruit from three fruits). From both the positive control and SA-treated samples, tissue from the lesions' margin (labeled as MLP and SAMLP, respectively; collected within 0.5 cm of the visible lesion's boundary) and newly rotted tissue (labeled NRP and SANRP, respectively; collected 1.0−1.5 cm from the lesion's margin) were collected. In the negative control group, where no disease developed, healthy tissues (HT, located 0.5−1.5 cm from the inoculation site) were collected.

Untargeted metabolomic analysis was performed on an ultrahigh-performance liquid chromatography coupled with quadrupole time-of-flight mass spectrometry (UPLC-Q-TOF/MS) platform (AB Triple TOF 6600) equipped with a HILIC column[15,17]. Frozen samples (80 mg) were extracted with 1 mL ice-cold acetonitrile (ACN) : MeOH : H_2O (2:2:1, v/v) via ultrasonication (4 °C, 1 h) and incubated at −20 °C for 1 h, followed by centrifugation (14,000 × *g*, 20 min, 4 °C). The supernatants were dried, reconstituted in 200 μL of the solvent, filtered (0.22 μm), and analyzed alongside quality control (QC) samples prepared by pooling aliquots from all extracts. Separation was achieved using a 12-min gradient elution (0.3 mL/min) with acetonitrile (A) and 25 mM ammonium acetate/ammonia in water (B) as the mobile phases. The column temperature was maintained at 25 °C, and the injection volume was 5 μL. Mass spectrometry detection was conducted in both electrospray ionization $(ESI)^+$ and ESI^- modes with the following parameters: Ion source temperature, 600 °C; spray voltage, ±5,500 V; and mass scan range *m/z*, 60−1,000. A QC sample was injected after every five experimental samples, and the system was calibrated using standard compounds from AB SCIEX.

For untargeted metabolomic data, raw files in mzXML format were processed using ProteoWizard software. Chromatographic peak extraction and alignment were performed with SCIEX OS and XCMS, respectively. Metabolite identification was achieved by matching the precursors' and products' ion spectra against a self-built database managed by Shanghai Applied Protein Technology Co., Ltd. in China.

Differential metabolites were defined as those with a variable importance in projection (VIP) > 1 from orthogonal partial least squares-discriminant analysis (OPLS-DA) and a $p < 0.05$ from Student's *t*-test[18]. These differential metabolites were subsequently subjected to Kyoto Encyclopedia of Genes and Genomes (KEGG) pathway enrichment analysis (www.kegg.jp) to identify relevant metabolic pathways[19]. Shared and group-specific metabolites were visualized using Venn diagrams generated with Mothur software (v.1.36.1).

Expanded sample collection and preparation for phenolic analysis

To validate the generalizability of the metabolomic findings, we used multiple *P. expansum* strains and apple fruits from diverse geographical origins. In total, 50 *P. expansum* strains, sourced from our previous research (details in Supplementary Table S1)[20] and apple samples collected from various domestic production regions (Supplementary Table S2) were used. Apple inoculation followed the procedure described in Section 'SA treatment and P. expansum inoculation of apples'. The lesions' diameters were measured on Days 5 and 10 after inoculation. Tissue samples from the lesion's margin (MLP) and healthy control tissues (HT) were collected using the same protocol. Samples were ground in liquid nitrogen and stored at −20 °C until analysis.

Phenolic compounds were extracted following a published method with slight modifications[21]. Briefly, a frozen sample (10.0 g) was mixed with 35 mL of methanol, and extracted at room temperature for 1 h. After centrifugation at 12,000 × *g* for 5 min, the supernatant was collected and made up to a final volume of 50 mL with methanol. A 5-mL aliquot of the extract was concentrated to dryness using a rotary evaporator. The residue was redissolved in methanol, purified by passing through a Sep-Pak C18 solid-phase extraction column (Waters, USA) and a 0.22-μm microporous filter membrane, and then prepared for instrumental analysis.

High-performance liquid chromatography analysis of phenolic compounds

Twelve phenolic compounds were analyzed: Protocatechuic acid, catechin, procyanidin B1, procyanidin B2, phloridzin, epicatechin, phloretin, chlorogenic acid, caffeic acid, *p*-coumaric acid, ferulic acid, and rutin (all from Extrasynthese, France). Standard stock solutions of each compound were prepared by accurately weighing 0.005 g of the compound, dissolving it in chromatographic-grade methanol, and diluting to 10 mL. These solutions were then serially diluted to concentrations of 0.5, 5, 20, 50, 80, and 120 mg/L to generate calibration curves. A mixed standard solution was prepared by combining the individual stock solutions in appropriate proportions.

Phenolic compounds were analyzed using a Shimadzu LC-20A high-performance liquid chromatography (HPLC) system (Japan) equipped with a Prominence SPD-M20A PDA detector. Separation was achieved on an XSelect HSS T3 column (4.6 mm × 250 mm, 5 μm; Waters, USA). Detection wavelengths were set at 280, 320 and 360 nm. The mobile phases consisted of (A) 5% formic acid in water

and (B) acetonitrile, with the following gradient elution program: 0–13 min, 5% B; 13–15 min, 5%→10% B; 15–18 min, 10%→15% B; 18–20 min, 12%→100% B; re-equilibration for 20–25 min, 5% B. The column temperature was maintained at 40 °C, with a flow rate of 1.0 mL/min and an injection volume of 3 μL. Quantification was performed using the external standard method. Total phenolic content was calculated as the sum of the individual components and expressed as mg/kg of fresh weight.

Statistical analysis

For phenolic compounds analysis, data were processed in Microsoft Excel. Statistical analysis was performed using SPSS software (version 26.0), with one-way analysis of variance (ANOVA) followed by Duncan's multiple range test to assess significant differences ($p < 0.05$) between treatment groups[22]. Pearson's correlation analysis was conducted to evaluate the relationships between phenolic compound contents and disease resistance indicators.

Results

SA treatment slows disease progression in apples

In SA-treated apples, the pathogen-induced lesion expanded more slowly than in the control. Daily measurements revealed consistently significant differences in diseased lesions' diameter ($p < 0.05$) between the two groups (Fig. 1b). By Day 10 after inoculation, the lesions' diameter in the SA-treated group measured 3.15 ± 0.16 cm, compared with 3.76 ± 0.20 cm in the positive control group ($p < 0.001$), confirming that SA significantly delayed blue mold's progression.

Lesions in SA-treated fruit were also markedly darker than the relatively lighter lesions in the control, suggesting that color-associated metabolic alterations are closely linked to disease progression (Fig. 1c). On the basis of these phenotypic observations, tissue samples from lesion margins and adjacent healthy areas were collected for subsequent untargeted metabolomic analysis to compare metabolic profiles associated with SA-induced disease resistance.

Untargeted metabolomics reveals marked changes in phenolic metabolism during disease development

During the 12-min chromatographic run, the total ion chromatograms (TICs) obtained in both ESI^+ and ESI^- modes showed that the dominant peaks had retention times ranging from 0.3 to 9.0 min. The differing TIC profiles highlighted marked alterations in the metabolic patterns across samples. Specifically, infection by *P. expansum* progressively increased the number of detected peaks in fruit tissues, following the order HT < MLP < NRP and SAMLP < SANRP ($p < 0.05$). In contrast, SA treatment caused a modest, nonsignificant rise in peak numbers for the corresponding samples (SAMLP > MLP, SANRP > NRP). QC samples were analyzed to assess the reliability of detection. QC runs produced reproducible TICs in both modes, and over 70% of the peaks exhibited consistent signal responses with a relative standard deviation (RSD) ≤ 30%. Principal component analysis (PCA) clustered all QC samples together while clearly separating them from the other experimental samples, indicating stable and consistent instrumental performance. Subsequent peak alignment between the ESI^+ and ESI^- datasets enabled a comparative analysis of the peaks and metabolites across samples, thereby capturing metabolite variations related to disease progression and SA treatment.

Untargeted metabolomic analysis identified 103 differentially abundant secondary metabolites among the five groups (Supplementary Table S3). A list of metabolites and their abundances for

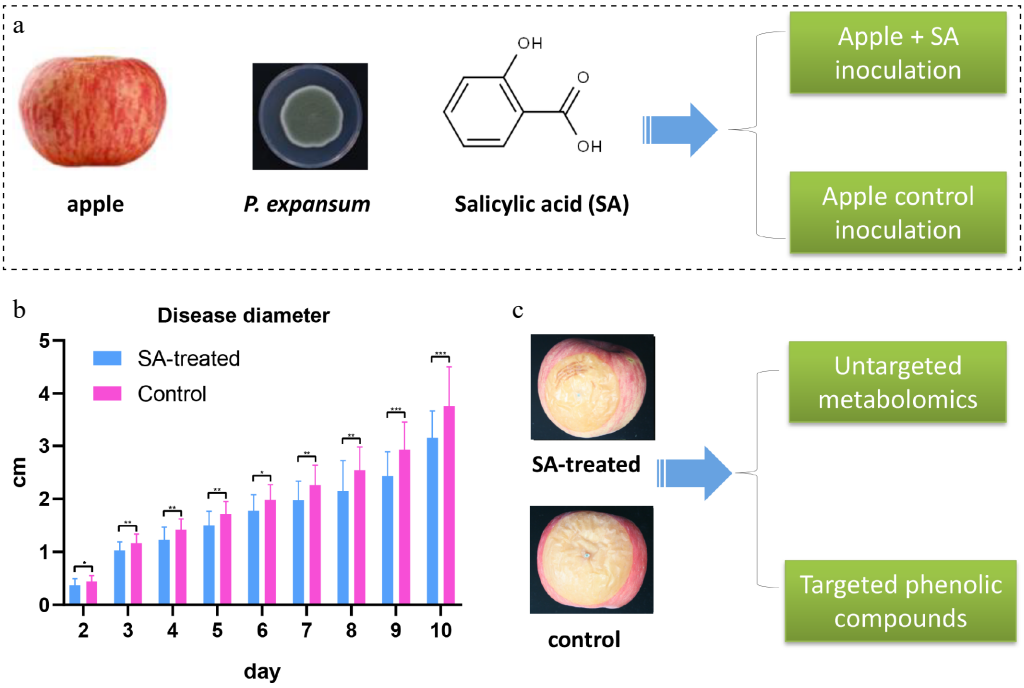

Fig. 1 Experimental workflow illustrating apple sample groupings, salicylic acid (SA) treatment, pathogen inoculation, disease assessment, and metabolomic analysis. (a) Schematic illustration of the SA treatment (pre-treated with 5 mmol/L SA followed by inoculation) and the control. (b) Statistical comparison of lesion diameters between the control and SA-treated groups (* $p < 0.05$, ** $p < 0.01$, *** $p < 0.001$). (c) Both control and SA-treated fruits were subjected to untargeted metabolomic analysis. Key differential metabolites were subsequently validated via targeted metabolomics using an expanded sample set.

https://doi.org/10.48130/ph-0026-0018

each sample, ranked by relative content, is presented in Fig. 2a. Compared with the HT samples, the relative abundance of 61 metabolites was generally increased and that of 42 was decreased in the infected samples. Among the top 10 most abundant metabolites, seven were found to be upregulated in infected samples, including caffeic acid, icariside i, calphostin c, 3-methylbenzyl alcohol, quercetagetin-7-O-glucoside, procyanidin a2, and nodakenin (Fig. 2a). Notably, the elevation in the levels of phenolics was more pronounced in SA-treated samples than in the infected control, suggesting that alterations in phenolic metabolism represent an important pathway through which SA enhances disease resistance in apple.

Based on the overall secondary metabolites, OPLS-DA revealed clear separation among sample groups, indicating distinct metabolic reprogramming under *P. expansum* infection and SA treatment (Fig. 2b). Specifically, HT samples were completely separated from infected samples, and SA-treated samples were also largely separated from the positive control samples. Validation plots from the permutation tests displayed regression lines with negative intercepts, and all permuted R^2 values were lower than the original values, confirming the model's robustness and reliability (Fig. 2c). Therefore, the OPLS-DA results clearly demonstrate the differences in metabolites between samples, reflecting the metabolic changes related to disease progression in apple. Furthermore, these results suggest that SA modulates these metabolic responses, steering disease progression by triggering systemic metabolic reprogramming in infected apple fruit.

KEGG analysis revealed that the differential metabolites were primarily enriched in several major metabolic pathways (Fig. 3a). Significantly enriched pathways included flavonoid biosynthesis, phenylpropanoid biosynthesis, flavone and flavonol biosynthesis, phenylalanine metabolism, and ubiquinone and other terpenoid-quinone biosynthesis. Among these, flavonoid and phenolic compound metabolism appeared to be the most prominent. Heatmap analysis of the associated metabolites revealed a distinct accumulation pattern. Major metabolites were observed with significantly higher levels in the SA-treated groups (SAMLP and SANRP) compared with the positive controls (Fig. 3b). This indicates that SA treatment markedly enhances the abundance of these compounds, contributing to the observed improvement in disease resistance.

HPLC analysis reveals differential trends of phenolic compounds during disease progression

To verify the generalizability of the aforementioned metabolic changes, we expanded the diversity of pathogen strains and apples' geographical origins. Targeted metabolomic analysis measured phenolic compound concentrations in 50 apple samples before and after *P. expansum* infection (Supplementary Table S4). Generally, the original HT samples contained higher levels of catechin, epicatechin, and chlorogenic acid, whereas MLP samples accumulated higher levels of caffeic acid, protocatechuic acid, and ferulic acid (Fig. 4).

Six compounds, namely caffeic acid, *p*-coumaric acid, protocatechuic acid, rutin, ferulic acid, and procyanidin B2, increased significantly in infected tissues ($p < 0.01$), reflecting their accumulation during the disease resistance process. Phloretin also exhibited a moderate increase in MLP tissues, though this was not statistically significant. In contrast, chlorogenic acid, phloridzin, procyanidin B1, catechin, and epicatechin decreased in infected tissues, reflecting enhanced catabolism. The metabolic changes varied by compound type, with some metabolites showing increasing concentrations and others showing decreasing concentrations. Taken together, these results systematically reveal the differential metabolic dynamics of phenolic compounds in apples in response to *P. expansum* infection.

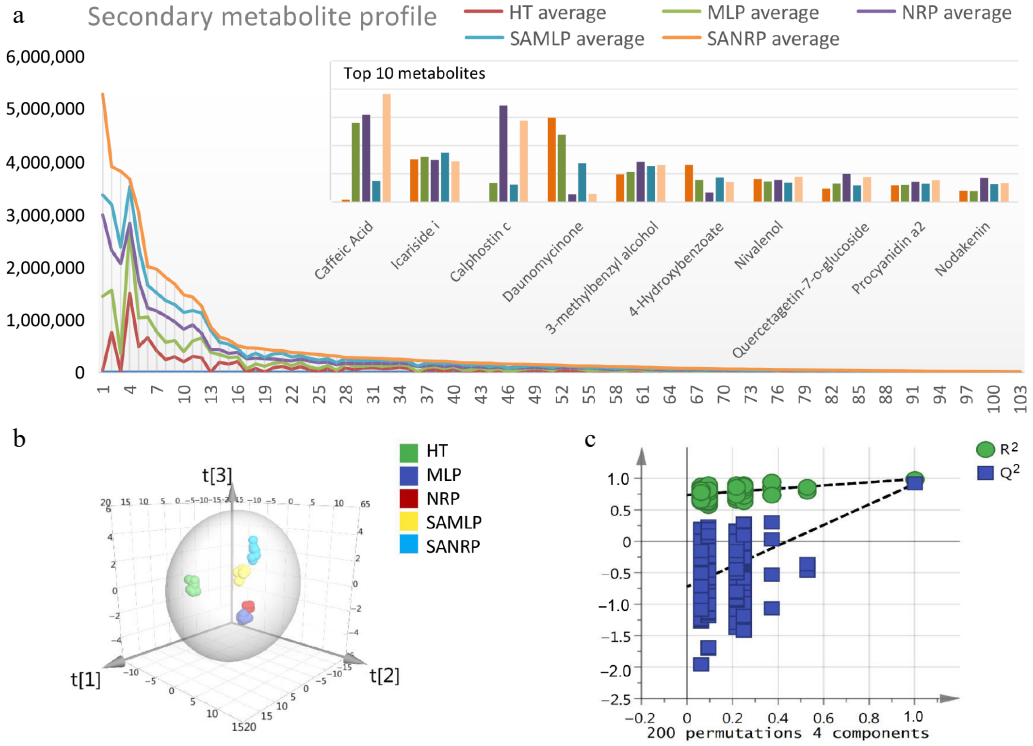

Fig. 2 Analysis of secondary metabolite profiles in apple fruit during *P. expansum* infection using OPLS-DA. (a) Secondary metabolite profiles in different tissue groups: Healthy tissue (HT), the lesion's margin (MLP), newly rotted tissue (NRP), and their SA-treated counterparts (SAMLP and SANRP). (b) Distinct group separation as visualized by the OPLS-DA model. (c) Permutation test validation plot confirming the robustness and reliability of the statistical model.

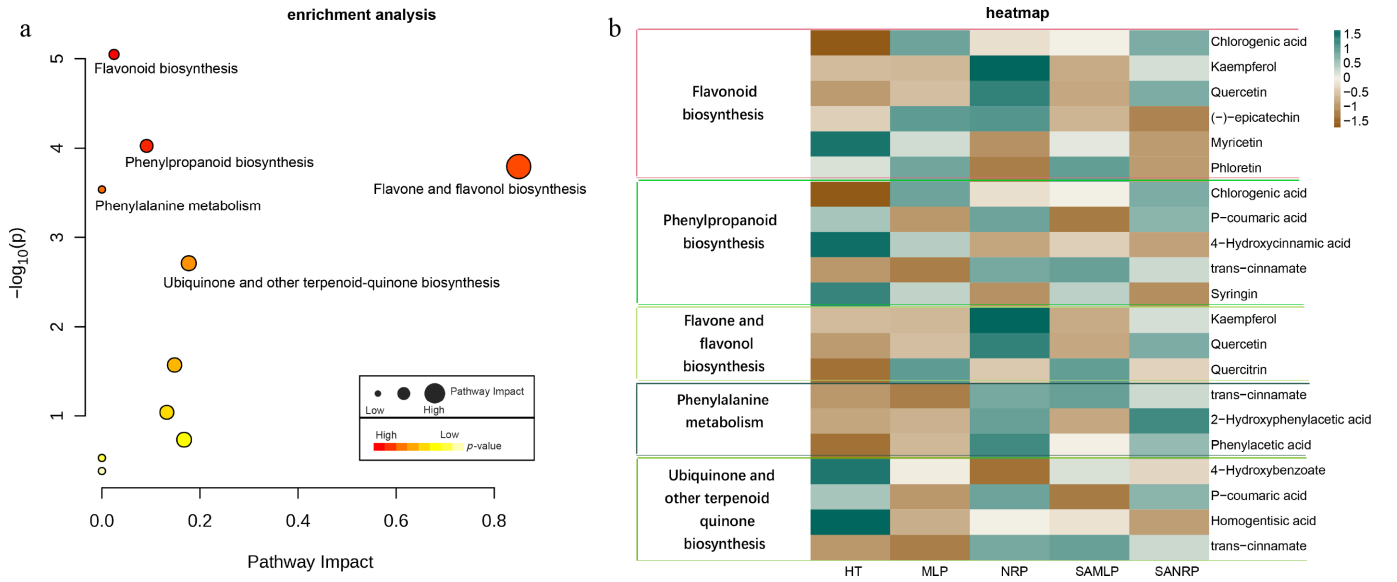

Fig. 3 KEGG pathway analysis of differential metabolites during *P. expansum* infection. (a) Enriched metabolic pathways. The color gradient from red to green indicates the level of significance [$-\log_{10}$ (*p*-adjust), with red representing higher significance], and the size of the dots represents the number of annotated metabolites. (b) Heatmap showing the relative abundance profiles of key differential metabolites across sample groups (HT, MLP, NRP, SAMLP, SANRP). Metabolite names are listed on the right. The color scale from blue to red represents the normalized abundance (Z-score).

Correlation between diseased lesions' diameter and phenolic metabolites

The correlations between the lesions' diameters and phenolic metabolite concentrations in HT and MLP samples were reflected in an overall correlation heatmap (Fig. 5a). Generally, metabolites showing positive correlations clustered together, separated from those showing negative correlation. As a result, these metabolites were grouped into three main clusters. Cluster 1 included catechin (in both the HT and MLP samples), epicatechin and procyanidin B2 (in the MLP samples), and phloridzin (in both the HT and MLP samples). Cluster 2 consisted entirely of metabolites in the MLP samples: Rutin, p-coumaric acid, procyanidin B1, protocatechuic acid, phloretin, caffeic acid, and chlorogenic acid. Cluster 3 contained metabolites found only in the HT samples: Procyanidin B1, procyanidin B2, chlorogenic acid, caffeic acid, and epicatechin. A strong negative correlation was observed between Cluster 1 and Cluster 3, reflecting the distinct distribution patterns of phenolic compounds between HT and MLP tissues. Lesion diameters measured on Days 5 and 10 fell between Clusters 1 and 2 and were positively correlated with the phenolic metabolite concentrations in the MLP samples.

Further analysis showed that eight compounds in MLP samples were positively correlated with the lesions' diameter, namely phloridzin, catechin, procyanidin B2, ferulic acid, rutin, p-coumaric acid, procyanidin B1, and protocatechuic acid (Fig. 5b), indicating a general increase of these compounds as the lesions expanded. In contrast, procyanidin B1, procyanidin B2, caffeic acid, chlorogenic acid, and epicatechin, which were primarily detected in HT samples, showed a negative correlation with lesion diameter. Thus, correlation analysis clarifies the close link between changes in phenolic compounds and expansion of the lesions.

Discussion

Postharvest blue mold caused by *P. expansum* infection poses a major challenge to apple storage in China and causes substantial economic losses[4,23]. SA is widely recognized as a promising elicitor for enhancing fruits' defense responses against fungal infections[9]. Understanding the metabolic reprogramming underlying SA-induced resistance is therefore essential for deciphering the disease's pathology and developing novel control strategies[24]. Consistent with previous reports, our results confirm that SA treatment effectively suppresses *P. expansum* infection in apple fruit[8]. The distinct lesion coloration in SA-treated versus control fruits further suggests that metabolic alterations play a pivotal role in disease development. The darker lesions in SA-treated samples likely reflect enhanced accumulation of phenolic secondary metabolites involved in the defense response, providing representative samples for subsequent metabolomic analysis.

Using an untargeted metabolomic approach, we compared the metabolic profiles of HT samples collected from the uninfected control, MLP and NRP samples from the infected control, and the corresponding SA-treated samples (SAMLP and SANRP). Metabolic profiling demonstrated a marked increase in the overall abundance of secondary metabolites in infected tissues compared with healthy tissues, an effect that was further amplified in SA-treated groups relative to the untreated infected control[25]. OPLS-DA modeling confirmed significant differences in metabolic profiles among the sample groups, supporting the hypothesis that SA activates secondary metabolic pathways in apple fruit in response to pathogen infection[9]. KEGG analysis revealed that these metabolites were primarily enriched in flavonoid biosynthesis, phenylpropanoid biosynthesis, and flavone and flavonol biosynthesis, suggesting that these pathways are closely associated with the disease resistance process.

To validate the generality of these changes, we expanded the study using multiple *P. expansum* strains and apple samples from diverse geographical origins, and used HPLC-targeted methods to precisely quantify the phenolic compounds. The results confirmed that the metabolic profiles of healthy and infected tissues differ substantially, with notable shifts in metabolites' abundance. Specifically, structurally simpler phenolics, such as *p*-coumaric acid, protocatechuic acid, and caffeic acid, increased in infected tissues, likely caused by enhanced biosynthesis following activation of defense pathways[26,27]. Conversely, more complex compounds, including

https://doi.org/10.48130/ph-0026-0018

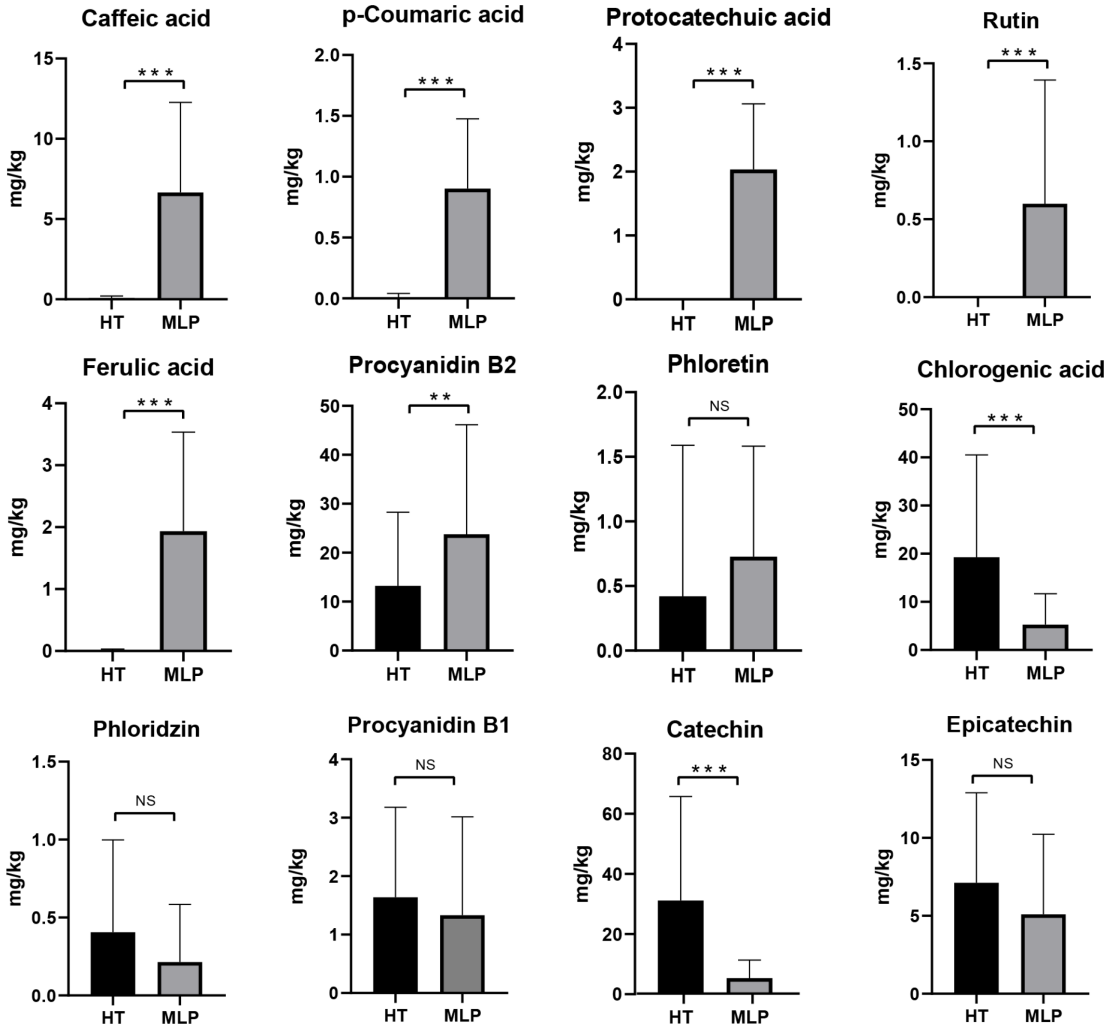

Fig. 4 Differential accumulation patterns of phenolic compounds in healthy (HT) and infected (MLP) apple tissues. Data are presented as mean ± standard deviation (SD). Compared with HT, the concentrations of caffeic acid, p-coumaric acid, protocatechuic acid, rutin, ferulic acid, procyanidin B2, and phloretin were elevated in MLP tissues. In contrast, the levels of chlorogenic acid, phloridzin, procyanidin B1, catechin, and epicatechin were reduced (** $p < 0.01$, *** $p < 0.001$; NS, nonsignificant differences).

procyanidins B1/B2 and chlorogenic acid, decreased in concentration in infected tissues, possibly because of fungal infection-mediated structural breakdown[28]. Notably, chlorogenic acid can be enzymatically degraded to caffeic acid, which may account for the observed rise in caffeic acid levels[29]. Given the direct association between these metabolic shifts and disease progression, we propose that the metabolic reprogramming represents a pivotal defensive response of the fruit against *P. expansum* invasion, playing a crucial role in the disease's pathogenesis.

Correlation analysis indicated that baseline levels of specific phenolic compounds in HT samples, particularly procyanidins B1/B2 and chlorogenic acid, were significantly negatively correlated with lesion diameter, suggesting these compounds contribute to basal disease resistance[26]. This insight could indicate fruits' resistance levels and aid in the breeding of resistant cultivars. In contrast, phenolic levels in MLP samples showed a positive correlation with lesion size, indicating that their accumulation might be a concomitant phenomenon of disease progression[30]. However, this correlation analysis only implies potential associations and does not confirm the functional role of these metabolites in the disease defense process. Consequently, future studies should prioritize validating the roles of these candidate metabolic pathways and characteristic bioactive compounds in mediating disease resistance.

Conclusions

This study demonstrates that SA effectively enhances apples' resistance to postharvest blue mold caused by *P. expansum* infection. By comparing the metabolic profiles between the SA-treated and control groups, we systematically identified 103 differentially accumulated secondary metabolites. Both infection and SA treatment significantly increased the overall abundance of secondary metabolites. KEGG analysis revealed metabolic reprogramming in apples associated with *P. expansum* infection and SA-mediated disease resistance. Targeted phenolic compound analysis validated the untargeted metabolomics findings and revealed distinct response patterns among phenolics of varying structural complexity. Notably, baseline levels of procyanidins B1/B2 and chlorogenic acid in healthy tissues showed a significant negative correlation with the lesions' expansion, suggesting their contribution to basal disease resistance. Collectively, our results indicate that SA enhances resistance to *P. expansum* by regulating the phenolic metabolic network in apples, particularly through activation of biosynthetic pathways for defense-related secondary metabolites. This work deepens the understanding of the metabolic mechanisms underlying postharvest disease resistance in apples and provides a theoretical foundation and potential metabolic markers

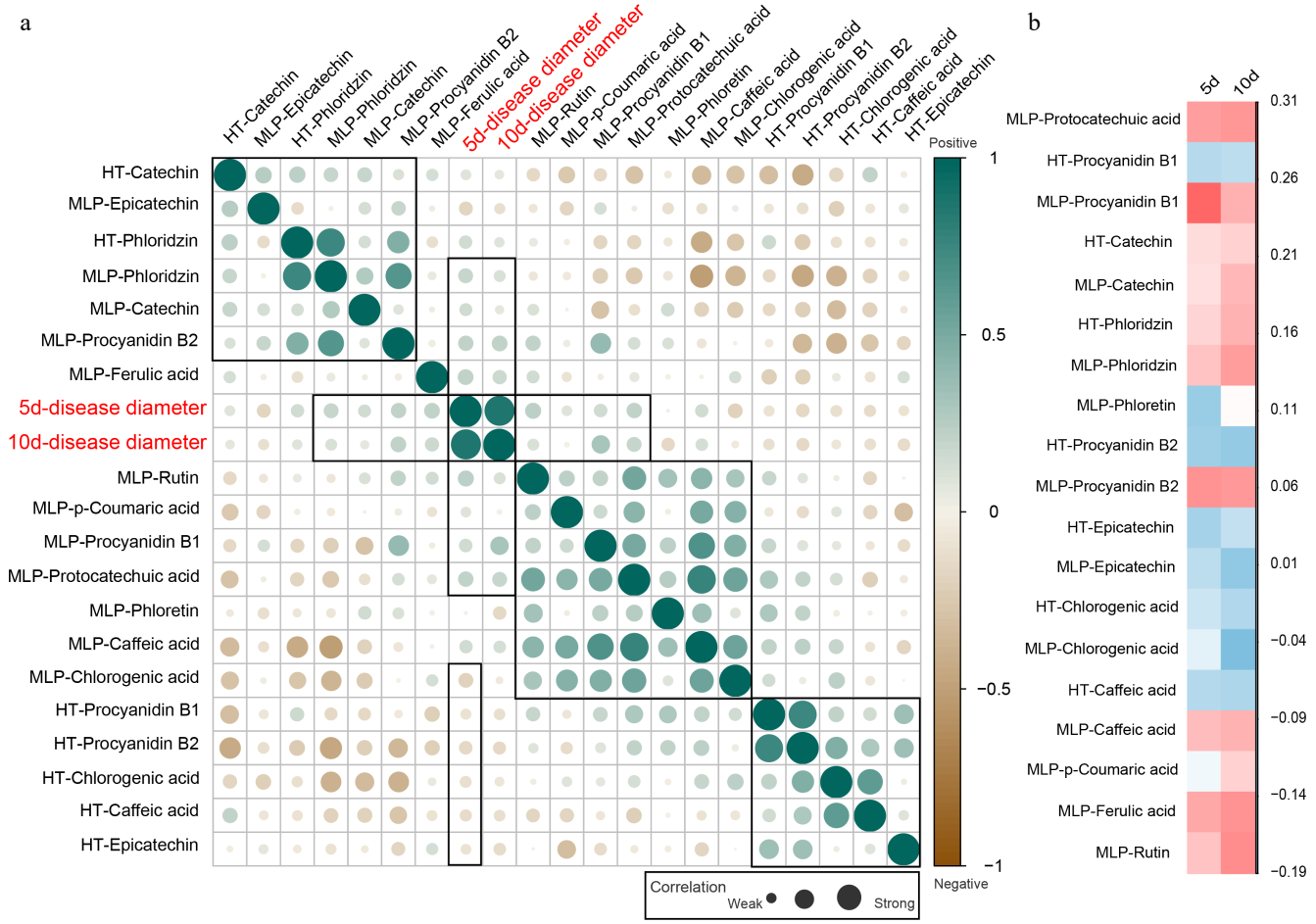

Fig. 5 Correlation analysis between disease progression and phenolic metabolite levels. (a) Correlation matrix between the lesions' diameters (measured on Days 5 and 10 after inoculation) and phenolic metabolites in healthy (HT) and infected (MLP) samples. Circle size represents the absolute correlation coefficient (|*r*|); larger circles indicate stronger correlations. (b) Heatmap visualization highlighting the correlations between the lesions' diameters and key phenolic metabolites in HT and MLP samples. The color scale from blue to red represents the strength and direction of the correlation (*Z*-score normalized).

for developing SA-based green preservation strategies and breeding apple cultivars with improved disease resistance. The findings thus offer a pathway toward translating fundamental research into practical postharvest management solutions.

Ethical statements

During the preparation of this work, the authors used Deepseek (r1) for language refinement. The authors reviewed and edited all content produced with the assistance of this tool, verified its accuracy, and take full responsibility for the integrity and originality of the final manuscript. This work represents the authors' own intellectual contribution, and no AI tool is credited as an author.

Author contributions

The authors confirm contribution to the paper as follows: study conception and design, draft manuscript preparation: Zhang J, Shen Y; data collection: Zhang J, Ji Z; analysis and interpretation of results: Shen Y, Ma N. All authors reviewed the results and approved the final version of the manuscript.

Data availability

The datasets generated during and/or analyzed during the current study are available from the corresponding author on reasonable request.

Acknowledgments

This work was supported by the Youth Innovation Program of Chinese Academy of Agricultural Sciences (Y2023QC26) and the Agricultural Science and Technology Innovation Program (CAAS-ASTIP).

Conflict of interest

The authors declare that they have no conflict of interest.

Supplementary information accompanies this paper online at: https://doi.org/10.48130/ph-0026-0018.

Dates

Received 16 April 2026; Revised 25 June 2026; Accepted 2 July 2026; Published online 26 August 2026

References

[1] Li M, Ma S. 2024. A review of healthy role of dietary fiber in modulating chronic diseases. *Food Research International* 191:114682

[2] Yang Y, He D, Wei L, Wang S, Chen L, et al. 2020. Association between diet-related knowledge, attitudes, behaviors, and self-rated health in Chinese adult residents: a population-based study. *BMC Public Health* 20:720

[3] Frisvad JC, Smedsgaard J, Larsen TO, Samson RA. 2004. Mycotoxins, drugs and other extrolites produced by species in *Penicillium* subgenus *Penicillium*. *Studies in Mycology* 49:201−241
[4] Zhu Y, Chen Y, Xing M, Romanazzi G, Tian S, et al. 2026. Volatile biomarkers of fungal infection and mycotoxin contamination in fruits and vegetables: emerging targets for monitoring and early warning. *Critical Reviews in Food Science and Nutrition* 66:2060−2073
[5] Shen Y, Ma N, Liu S, Xu G, Zhang J. 2025. Mycotoxins and secondary metabolites from fruit postharvest pathogenic *Penicillium* species. *Food Chemistry* 488:144880
[6] Szpyrka E, Migdal-Pecharroman S, Książek-Trela P. 2025. Biological strategies and innovations in pest control and fruit storage in apple orchards: a step towards sustainable agriculture. *Agronomy* 15:2373
[7] Xu Y, Liu Y, Wang H, Huo L, Shi H. 2025. Genome-wide analysis of TGACG motif-binding factor (TGA) family and mechanism of PpTGA2. 1-L and PpTGA7-L response to salicylic acid regulating fruit senescence through interaction with PpNPR1 in sand pear. *Postharvest Biology and Technology* 227:113615
[8] Zhang X, Liu Y, Zhang W, Yang W, An S, et al. 2024. Salicylic acid treatment ameliorates postharvest quality deterioration in 'France' prune (*Prunus* domestica L. 'Ximei') fruit by modulating the antioxidant system. *Foods* 13:2871
[9] Decsi K, Ahmed M, Abdul-Hamid D, Tóth Z. 2025. The role of salicylic acid in activating plant stress responses-results of the past decade and future perspectives. *International Journal of Molecular Sciences* 26:4447
[10] Ballester AR, Norelli J, Burchard E, Abdelfattah A, Levin E, Gonzalez-Candelas L, et al. 2017. Transcriptomic response of resistant (PI613981–*Malus sieversii*) and susceptible ('Royal Gala') genotypes of apple to blue mold (*Penicillium expansum*) infection. *Frontiers in Plant Science* 8:1981
[11] Dobón-Suárez A, Gutiérrez-Pozo M, Serna-Escolano V, Giménez MJ, Valero D, et al. 2025. Antioxidant metabolism insights into ripening and senescence delay of green pepper fruit through the salicylic acid preharvest treatment. *Frontiers in Plant Science* 16:1475068
[12] Cao H, Glazebrook J, Clarke JD, Volko S, Dong X. 1997. The *Arabidopsis* NPR1 gene that controls systemic acquired resistance encodes a novel protein containing ankyrin repeats. *Cell* 88(1):57−63
[13] Ferreira C, Ribeiro C, Nunes FM. 2024. Effect of storage conditions on phenolic composition, vitamin C and antioxidant activity of 'Golden Delicious' and 'Red Delicious' apples. *Postharvest Biology and Technology* 210:112754
[14] Chen L, Zhao X, Wu JE, He Y, Yang H. 2020. Metabolic analysis of salicylic acid-induced chilling tolerance of banana using NMR. *Food Research International* 128:108796
[15] Zhang J, Ma N, Xu G, Kuang L, Li Z, et al. 2024. Metabonomic investigation of *Penicillium expansum* infection of apples and salicylic acid-mediated disease resistance. *Food and Bioprocess Technology* 17:2869−2884
[16] Wang Y, Yang Q, Godana EA, Zhang Y, Zhang H. 2023. Ultrastructural observation and transcriptome analysis provide insights into mechanisms of *Penicillium expansum* invading apple wounds. *Food Chemistry* 414:135633
[17] Dunn WB, Erban A, Weber RJM, Creek DJ, Brown M, et al. 2013. Mass appeal: metabolite identification in mass spectrometry-focused untargeted metabolomics. *Metabolomics* 9:44−66
[18] Navarro-Herrera AM, Rivera-Pérez A, Belmonte-Sánchez JR, Garrido Frenich A. 2025. Innovative SALLE-GC-Orbitrap-HRMS-based metabolomics and multi-technique data fusion: a combined approach for botanical marker identification of monofloral and multifloral honey. *Food Chemistry* 495:146418
[19] Kanehisa M, Goto S. 2000. KEGG: kyoto encyclopedia of genes and genomes. *Nucleic Acids Research* 28:27−30
[20] Shen Y, Ma W, Ma N, Li M, Zhang J, et al. 2024. Genetic identification, pathogenicity and patulin production of *Penicillium* species from apple blue mold in China. *Food Quality and Safety* 8:fyad073
[21] Li SY, He F, Zhu BQ, Xing RR, Reeves MJ, et al. 2016. A systematic analysis strategy for accurate detection of anthocyanin pigments in red wines. *Rapid Communications in Mass Spectrometry* 30:1619−1626
[22] Sun LN, Wang GW, Qi YL, Cui KB, Ma Y, et al. 2025. Comprehensive characterization of physicochemical quality and volatile organic compounds of walnut oil under different treatment conditions based on HS-GC-IMS and chemometrics. *Food Chemistry: Advances* 9:101141
[23] Ngolong Ngea GL, Yang Q, Xu M, Ianiri G, Dhanasekaran S, et al. 2024. Revisiting the current and emerging concepts of postharvest fresh fruit and vegetable pathology for next-generation antifungal technologies. *Comprehensive Reviews in Food Science and Food Safety* 23:e13397
[24] Jiang B, Liu R, Fang X, Tong C, Chen H, et al. 2022. Effects of salicylic acid treatment on fruit quality and wax composition of blueberry (*Vaccinium virgatum* Ait). *Food Chemistry* 368:130757
[25] Romanazzi G, Sanzani SM, Bi Y, Tian S, GutiérrezMartínez P, et al. 2016. Induced resistance to control postharvest decay of fruit and vegetables. *Postharvest Biology and Technology* 122:82−94
[26] Sun Y, Wang X, Huang Z, Zhao X, Qiao L, et al. 2025. Phenylpropanoids for the control of fungal diseases of postharvest fruit. *Plant Molecular Biology* 115:39
[27] Zhang S, Gai Z, Gui T, Chen J, Chen Q, et al. 2021. Antioxidant effects of protocatechuic acid and protocatechuic aldehyde: old wine in a new bottle. *Evidence-Based Complementary and Alternative Medicine* 2021:6139308
[28] Raynaldo FA, Xu Y, Yolandani, Wang Q, Wu B, et al. 2024. Biological control and other alternatives to chemical fungicides in controlling postharvest disease of fruits caused by *Alternaria alternata* and *Botrytis cinerea*. *Food Innovation and Advances* 3(2):135−143
[29] Lin Q, Chen J, Liu X, Wang B, Zhao Y, et al. 2023. A metabolic perspective of selection for fruit quality related to apple domestication and improvement. *Genome Biology* 24:95
[30] Žebeljan A, Vico I, Duduk N, Žiberna B, Urbanek Krajnc A. 2019. Dynamic changes in common metabolites and antioxidants during *Penicillium expansum*-apple fruit interactions. *Physiological and Molecular Plant Pathology* 106:166−174